Thermodynamics of Reversible Monomer-Dimer Association of Tubulin

Dan L. Sackett* and Roland E. Lippoldt

Building 10, Room 8N308, National Institute of Diabetes, Digestive, and Kidney Diseases, National Institutes of Health, Bethesda, Maryland 20892

Received May 11, 1990; Revised Manuscript Received December 11, 1990

ABSTRACT: The equilibrium between the rat brain tubulin $\alpha\beta$ dimer and the dissociated α and β monomers has been studied by analytical ultracentrifugation with use of a new method employing short solution columns, allowing rapid equilibration and hence short runs, minimizing tubulin decay. Simultaneous analysis of the equilibrium concentration distributions of three different initial concentrations of tubulin provides clear evidence of a single equilibrium characterized by an association constant, K_a, of 4.9×10^6 M^{-1} ($K_d = 2 \times 10^{-7}$ M) at 5 °C, corresponding to a standard free energy change on association $\Delta G° = -8.5$ kcal mol^{-1}. Colchicine and GDP both stabilize the dimer against dissociation, increasing the K_a values (at 4.5 °C) to 20×10^6 and 16×10^6 M^{-1}, respectively. Temperature dependence of association was examined with multiple three-concentration runs at temperatures from 2 to 30 °C. The van't Hoff plot was linear, yielding positive values for the enthalpy and entropy changes on association, $\Delta S° = 38.1 \pm 2.4$ cal deg^{-1} mol^{-1} and $\Delta H° = 2.1 \pm 0.7$ kcal mol^{-1}, and a small or zero value for the heat capacity change on association, $\Delta C_p°$. The entropically driven association of tubulin monomers is discussed in terms of the suggested importance of hydrophobic interactions to the stability of the monomer association and is compared to the thermodynamics of dimer polymerization.

Microtubules can self-assemble from tubulin dimers without the participation of associated proteins. In investigations of this polymerization reaction the dimer is considered to be the unit of assembly even though it is itself an equilibrium structure between the similar but nonidentical α and β tubulin monomers. Each monomer is composed of a larger amino and a smaller carboxy globular domain and a highly charged, carboxy-terminal "tail" (Sackett & Wolff, 1986). The intradimer contact region appears to involve the amino domain of α tubulin, α·N, and the carboxy domain of β tubulin, β·C (Kirchner & Mandelkow, 1985; Serrano & Avila, 1985).

The reversible dissociation of the bovine brain tubulin dimer was demonstrated by equilibrium ultracentrifugation and shown to be consistent with a dissociation constant, K_d, of $(8-10) \times 10^{-7}$ M at 4.6 °C (Detrich & Williams, 1978; Detrich et al., 1982). A similar value was obtained from fluorescence anisotropy measurements, yielding a K_d of 8.4×10^{-7} M (Mejillano & Himes, 1989), and from spectral changes in the fluorescence of Nile Red, which indicated a K_d of ca. 10×10^{-7} M (Sackett et al., 1990). We were surprised, therefore, when another type of measurement of this equilibrium, relying on the increased exposure of a subtilisin cleavage site on β tubulin in the monomer compared to the dimer, yielded a K_d of 1.5×10^{-7} M at 5 °C (Sackett et al., 1989a). This difference in the K_d values appeared to exceed the technical errors of the methods. Because there were potential problems of tubulin decay during the long times required to attain equilibrium in the earlier centrifugation experiments (Detrich et al., 1982), we have reinvestigated the monomer-dimer equilibrium of pure rat brain tubulin by a novel equilibrium centrifugation method that employs very short solution columns, thus allowing short equilibration times during which decay of tubulin could be kept to a minimum. We have also used this method to study the thermodynamics of dimerization because a comparison with existing data on polymerization might reveal similarities between intradimer and interdimer (longitudinal) contact.

* To whom correspondence should be addressed.

Materials and Methods

Tubulin was isolated by phosphocellulose chromatography of microtubule protein purified from rat brain by two cycles of temperature-dependent polymerization and depolymerization in Mes[1] assembly buffer [0.1 M 2-(*N*-morpholino)-ethanesulfonic acid (Mes), 1 mM $MgCl_2$, and 1 mM EGTA, pH 6.9] with 1 mM GTP (Shelanski et al., 1973; Sloboda & Rosenbaum, 1982). Some tubulin was purified by cycling microtuble protein in PIPES/DMSO followed by glutamate (Himes et al., 1977; Hamel & Lin, 1984). Protein was stored in liquid nitrogen, following drop freezing in liquid nitrogen.

Tubulin–GDP complex was prepared by taking advantage of the Mg^{2+} dependence of guanine nucleotide binding to tubulin (Croom et al., 1985; Correia et al., 1987). Briefly, tubulin was diluted to about 1 mg/mL in Mes (0.1 M)/EGTA (0.5 mM)/EDTA (0.5 mM)/GDP (0.1 mM), pH 6.9 and desalted into the same buffer minus EDTA with use of Bio-Gel P10 (see below). GDP was added to 1 mM and the solution incubated at room temperature for 30 min. $MgCl_2$ was added to 1 mM and the solution desalted into Mes assembly buffer plus GDP (0.02 mM) and DTT (0.2 mM).

Tubulin–colchicine complex was prepared by diluting tubulin to about 1 mg/mL in Mes assembly buffer and adding colchicine to 1 mM. The solution was incubated for 45 min at room temperature and desalted into Mes assembly buffer plus DTT (0.2 mM). All desalting steps in preparation of tubulin–GDP or tubulin–colchicine were performed by centrifugal desalting (Andersen & Vaughan, 1982; Christopherson, 1983). The 0.1-mL sample was centrifuged (1500*g* for 30 s) over a 0.6–0.7-mL minicolumn of Bio-Gel P10 (Bio-Rad Laboratories, Richmond, CA) equilibrated in the appropriate buffer and prepared in small filter tubes suitable

[1] Abbreviations: Mes, 2-(*N*-morpholino)ethanesulfonic acid; EGTA, ethylene glycol bis(β-aminoethyl ether)-*N*,*N*,*N*′,*N*′-tetraacetic acid; EDTA, ethylenediaminetetraacetic acid; DMSO, dimethyl sulfoxide; DTT, dithiothreitol; α·N, amino domain of α tubulin; α·C, carboxy domain of α tubulin; β·N, amino domain of β tubulin; β·C, carboxy domain of β tubulin.

for use in a table-top microcentrifuge (Costar "Spin-X", No. 8162, Cambridge, MA).

Protein concentration was determined by optical density with an extinction coefficient (at 278 nm) of 1.23 mL mg^{-1} cm^{-1} (Detrich & Williams, 1978) or by the bicinchoninic acid (BCA) method (Pierce Chemical Co., St. Louis, MO) with bovine serum albumin as a standard. We found that tubulin concentration determined in this way gave values very close to those obtained using the extinction coefficient at 278 nm given above or to those obtained upon dilution in 6 M guanidine hydrochloride and employing an extinction coefficient (at 275 nm) of 1.09 mL mg^{-1} cm^{-1} (Andreu & Timasheff, 1982). Since the slit width on the ultracentrifuge is quite broad (2 mm, yielding a bandwidth of about 10–20 nm centered at 280 nm), we empirically determined an extinction coefficient for use in the centrifuge studies. This was done by taking several solutions of tubulin of known concentration, centrifuging them at low speed, and measuring the absorbance scanner optical density. This gave an empirical (monomer) extinction coefficient of 5.36×10^4 L mol^{-1} (assuming the extinction coefficients of monomer and dimer do not differ and assuming monomer mass of 54 kDa).[2]

Analytical ultracentrifugation was performed with a Beckman Model E analytical ultracentrifuge equipped with a xenon arc light source, a Beckman DU monochromator, the standard Beckman absorbance scanner, and the data collection system described below. All runs utilized 12-mm, double-sector scanner cells with quartz windows and were typically performed by using a Ti AN-F 4 place rotor. Samples were prepared at three different concentrations in Mes assembly buffer with 1 mM DTT. Samples (typically 50 μL) were loaded into nitrogen-flushed cells, followed by a further nitrogen flush prior to sealing. The rotor was accelerated to 32 000 rpm and maintained at this speed for 1 h. Following this period of overspeeding, the rotor was decelerated (with medium braking) to 26 000 rpm and maintained at this speed until equilibrium was demonstrated (typically the total run time was <3 h). Equilibrium was demonstrated as described below. Rotor temperature was measured on an instrument manufactured by Arden Instruments (similar to Beckman's RITC, rotor temperature indicator and controller) that was calibrated against a National Bureau of Standards traceable thermometer.

Data collection was accomplished with use of the digital data collection system described by Sackett et al. (1989b). This system converts each sample scan of the absorbance scanner to digital data files that can be directly analyzed by standard spreadsheet software. Briefly, the system consists of the centrifuge scanner, an interface circuit, an analog to digital converter and integrator, and a personal computer. The input voltage to the scanner strip chart recorder is passed through an interface circuit that conditions the signal. This is used as input to the analog to digital converter (a CHROM-1 board (MetraByte Corp., Taunton, MA), which integrates the signal for a user-selectable time interval (in our case, 20 ms) and writes the data to a file on a floppy disk in the computer. With this system, date density of 200 points/mm of solution column height (about 5 points/μL of sample) is easily achieved.

Data analysis was performed in two stages. The first stage consisted of demonstration of equilibrium and averaging of multiple scans and was performed with Lotus 1-2-3, Rel. 2. Demonstration of equilibrium was performed by difference plots, made by subtracting one scan from one taken some time later [see Figure 2 in Sackett et al. (1989b)]. When the difference plot is randomly distributed around zero for two scans taken 30–40 min apart, the sample is at equilibrium. At equilibrium, multiple scans were taken of each cell in order to minimize random noise as well as systematic deviation due to rotor precession. These were simply averaged with the spreadsheet, and the file was trimmed for final analysis. (Trimming consisted of eliminating the meniscus, air–air portion of the scan, bottom of the cell, etc.) Final analysis of the data was performed on a DEC-10 computer following file transfer. Fitting to the equations detailed below was performed by nonlinear least-squares curve-fitting routines of MLAB (Modeling Laboratory, Division of Computer Research and Technology, National Institutes of Health, Bethesda, MD).

At sedimentation equilibrium, the concentration of any given molecule at radical position r is given by

$$c_r = c_b \exp[AM(r^2 - r_b^2)] \quad (1)$$

and the concentration of all molecular species at radial position r is given by

$$c_{t,r} = \sum c_{b,i} \exp[A_i M_i (r^2 - r_b^2)] + e \quad (2)$$

where for the ith species, $c_{b,i}$ refers to the concentration at the cell bottom (r_b), M_i = the molecular weight, and $A = [(1 - v_i\rho)\omega^2]/2RT$, where v_i is the partial specific volume of the ith species, ρ is the solution density, ω is the angular velocity, R is the gas constant, and T is the absolute temperature, and e is a base-line error term.

In the case of tubulin, the species present is a heterodimer, "xy", in equilibrium with the monomers, "x" and "y", according to the association constant $K_a = c_{xy}/c_x c_y$. Equation 2 can be rewritten with terms for x, y, and xy, or the term for the dimer contribution can be expressed in terms of the monomer concentrations and the association constant, K_a. Further simplification of terms is possible due to the conservation of mass, since $c_x = c_y$. If this is done and concentration terms are converted to optical density, we obtain

$$OD_r = 2[OD_{b,x} \exp(A_x M_x (r^2 - r_b^2)) + ((OD_{b,x})^2/E) \exp(\ln K + 2A_x M_x (r^2 - r_b^2))] + e \quad (3)$$

where M_x = monomer molecular weight, here taken as 54 000,[2] A_x refers to A calculated with the partial specific volume of the monomer, taken to equal that of the dimer, calculated (Cohn & Edsall, 1943) to be 0.725 with amino acid data from porcine brain tubulin (Ponstingl et al., 1984), and E is the molar extinction coefficient of the monomer, measured to be 5.36×10^4. It is assumed that $M_x = M_y$, $E_x = E_y = E_{xy}/2$, and $A_x = A_y$. Equation 3 can be expressed with all fitting parameters in logarithmic form, which avoids fittings with negative concentration or association constant value (Lewis & Youle, 1986). This yields the fitting function used for the nonlinear least-squares fitting of the data

$$OD_r = 2[\exp(\ln OD_{b,x} + A_x M_x (r^2 - r_b^2)) + \exp((2(\ln OD_{b,x})) - \ln (E) + \ln K + 2A_x M_x (r^2 - r_b^2))] + e \quad (4)$$

where ln K, ln $OD_{b,x}$ and e are the fitting parameters.

Results

Experimental Design and Data Treatment. Sedimentation equilibrium studies have been performed on solutions of tubulin in order to examine the reversible dissociation of the tubulin dimer and to determine the temperature dependence of the

[2] Although the deduced monomer molecular mass based on the amino acid sequence is 50 kDa, the experimental value obtained by a variety of techniques in solution is 54 kDa (Lee et al., 1973; Ponstingl et al., 1984).

monomer–dimer equilibrium. In order to do this, we have employed an experimental design that places stringent constraints on the data. A constraint is placed on the experiment by the nature of tubulin. Since tubulin is labile, experiments of long duration are complicated by the problem of tubulin decay (Detrich & Williams, 1978). We have attempted to minimize this by the use of small samples and hence short solution columns in the centrifuge with resulting rapid equilibration times. However, short columns limit the number of useable data points, and hence the quality of fit to the data. We have avoided this problem by the use of a high-data-density recording system and the use of three-cell simultaneous analysis. A short description of this follows.

The concentration distribution at sedimentation equilibrium of two molecules of differing mass will be identical if the two molecules are noninteracting or if they are in rapid equilibrium (given the same mole ratio in each case). The demonstration of a reversible equilibrium between the two species requires more data than can be obtained from a single run (Teller, 1973). The presence of a reversible equilibrium can be demonstrated by the use of multiple runs. If a single total concentration of protein, centrifuged to equilibrium at several different rotor speeds, yields concentration distributions that each require the same equilibrium constant or constants, or that equivalently result in a continuous plot of weight-average molecular weight versus concentration, then a reversible equilibrium between the components of the solution is demonstrated (Roark, 1976). Similarly stringent demonstrations of reversible equilibrium may be obtained by centrifuging several different initial concentrations to equilibrium at a single rotor speed and obtaining the same equilibrium constant for all distributions. The use of multiple concentrations at multiple rotor speeds is even more stringent (Roark, 1976).

We have used a slight modification of the last approach (multiple concentrations at multiple speeds). Each run consists of three concentrations of tubulin that are centrifuged in cells with differing radii, resulting in different relative centrifugal forces just as different rotor speeds would. The use of the data collection system described under Materials and Methods and in Sackett et al. (1989b) allowed very high data density (about 200 points across a 1-mm solution column, corresponding to an optical density measurement every 5 μm). The significance of this to experiments with tubulin is that this allowed the use of short solution columns and consequently short times to equilibrium (<3 h), minimizing problems of tubulin decay (Detrich & Williams, 1978). In addition, this system allowed the rapid demonstration of attainment of equilibrium, again minimzing run time (Sackett et al., 1989b).

The data from such an experiment could be analyzed in more than one way. Initially, each cell could be treated separately, the distribution from each cell being analyzed for the concentrations of each of the species present in the equilibrium, the equilibrium constant for that cell calculated, and compared with constants calculated similarly for each of the other cells. Alternatively, the data sets may be analyzed simultaneously, with an equilibrium constant common to all of the data sets as a fitting parameter. We have used the latter approach, since it avoids intermediate calculations, requires fewer parameters for the analysis, and can be constrained to yield physically meaningful parameter values and to account for conservation of mass [see Materials and Methods and Roark (1976), Williams (1979), and Lewis and Youle (1986)].

Demonstration of Attainment of Equilibrium. In order to avoid run times that needlessly extend beyond the equilibrium time, we have used the rapid difference plot method to demonstrate attainment of equilibrium (Sackett et al., 1989b). Figure 1 presents typical data. In both panel A and panel B data are plotted as volts (output voltage of the scanner) versus seconds (seconds of scan, from the outside to the inside of the rotor cell); insets provide conversion to radial distance and optical density. Panel A presents the equilibrium distribution of optical density versus radial position for a sample of tubulin centrifuged as detailed under Materials and Methods. Following reduction of speed to 26 000 rpm (defined as $t = 0$ in the discussison to follow), scans were taken at 30-min intervals. At equilibrium, subtraction of a scan taken at time t from one taken at time $t + \Delta t$ will yield a difference plot that is a straight line of near-zero value (small nonzero values may occur due to drift of the scanner base-line voltage). On the other hand, if sedimentation has continued during the interval Δt, the difference plot will differ systematically from the equilibrium result; i.e., positive values will be obtained near the cell bottom and negative values nearer to the meniscus. Panel B shows the difference plot (note that the ordinate scale in panel B is expanded compared to panel A). Curve 1 shows the difference between scans taken at $t = 30$ min and $t = 0$ (rotor speed reaches 26 000 rpm). Clearly some sedimentation has occurred during this period. Curve 2 shows the difference between scans taken at 60 and 30 min. Little or no further

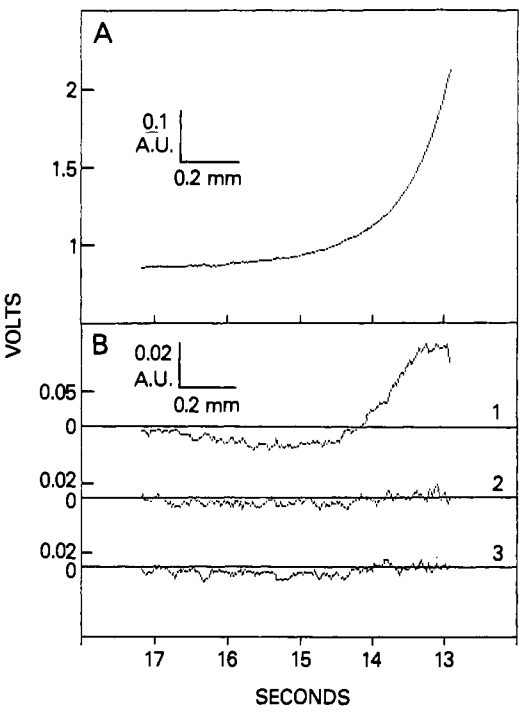

FIGURE 1: Attainment of sedimentation equilibrium. Tubulin solutions were prepared in Mes assembly buffer + 1 mM DTT and loaded into centrifuge cells as described under Materials and Methods. In order to minimize run times, a combination of overspeeding with difference plot analysis was employed. A 50-μL aliquot of 0.12 mg/mL tubulin was centrifuged for 1 h at 32 000 rpm at 4.3 °C. Following this period of overspeeding, the rotor was adjusted to 26 000 rpm (here defined as $t = 0$), and scans were taken at 30-min intervals. Subtraction of a given scan from a subsequent one produces the difference plot. The portions of the scans near the meniscus (left) and the bottom of the cell (right) have been removed, leaving about 200 points for each scan. Raw data are shown, i.e., scanner output in volts, versus the seconds elapsed since the scanner passed the outer reference mark, moving from the outside to the inside of the cell. In addition, insets show the conversion to optical density and radial distance. Panel A shows the equilibrium distribution, taken at $t = 60$ min. Panel B shows the difference plots. Note that the ordinate scale is expanded relative to panel A. Curve 1 = the scan at $t = 30$ min minus the scan at $t = 0$. Curve 2 = the scan at $t = 60$ min minus the scan at $t = 30$ min. Curve 3 = the scan at $t = 150$ min minus the scan at $t = 30$ min.

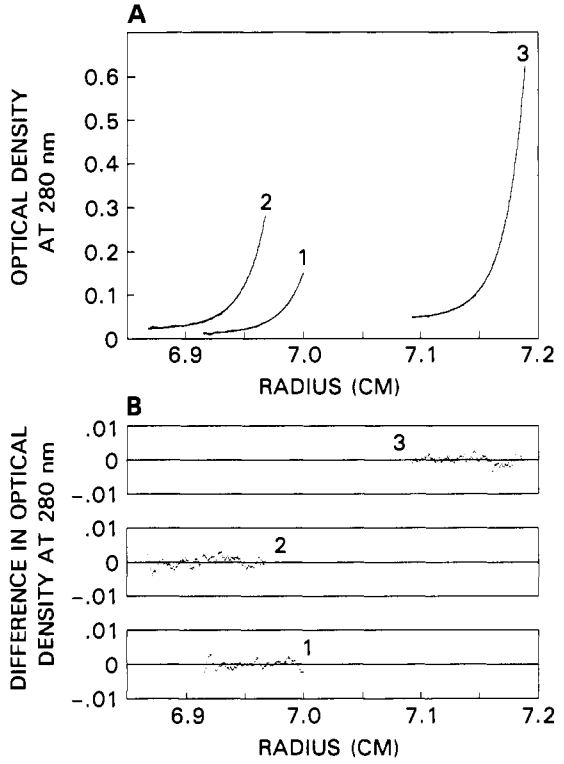

FIGURE 2: Absorbance scans and results of fit to the equilibrium sedimentation pattern of tubulin. Each equilibrium run consisted of three samples at different concentrations of tubulin that were centrifuged in cells with three different radii at the bottom of the cell (see text). Tubulin solutions were prepared in Mes assembly buffer + 1 mM DTT at three different concentrations: (1) 0.06 mg/mL; (2) 0.12 mg/mL; and (3) 0.3 mg/mL. Samples of 50 μL of each of these solutions were loaded into cells under nitrogen. Samples were then centrifuged to equilibrium at 26 000 rpm (see Materials and Methods). Multiple scans were collected and averaged for each cell and the data converted to optical density and radial position as described under Materials and Methods. The resulting data were simultaneously fitted to equations for the distribution of monomeric and dimeric tubulin, with the concentration of monomers and dimers in all cells governed by a common association constant, K_a, as described in detail under Materials and Methods. (A) Data from a three-cell run at 13.24 °C shown with the values from the fit. Data consist of about 200 points across each sample and are shown as dots. The global fit yielded an association constant, K_a, of 5.2×10^6 M^{-1}. On the basis of this K_a and the other details of the run, the expected distributions were calculated and are shown as solid lines. The concentrations of tubulin in the three cells correspond to about (1) 40%; (2) 30%; and (3) 20% dissociation calculated by using this *Ka*. (B) Residuals of the fit. The differences between the data and the corresponding values predicted from the globally fitted K_a were calculated for each cell and are shown as dots. Note the difference in scale on the ordinate compared to panel A. Calculated root mean square deviation error for this fit = 0.0013.

sedimentation has occurred during this period, implying that the sample was near equilibrium at 30 min. Curve 3 reinforces this point, showing the difference between scans at t = 30 min and t = 150 min. The additional 2 h of centrifugation resulted in negligible change in pattern. Thus, the sample was very near equilibrium at 30 min, the 60-min scan would be taken as equilibrium (panel A shows the 60-min scan), and data would be collected at this time from all three cells of a three-cell experiment as described under Materials and Methods.

Characterization of Monomer–Dimer Equilibrium. The results of a typical three-cell experiment are presented in Figure 2. Solutions of tubulin at three concentrations were prepared in Mes assembly buffer plus DTT and centrifuged to equilibrium. The three concentration distributions are shown with the results of the simultaneous fitting procedure in panel A. The fitting procedure yielded an association constant, K_a, of 5.2×10^6 M^{-1}, corresponding to a standard free energy change on association, $\Delta G° = -8.8$ kcal mol^{-1} by eq 6. The goodness of fit to the data is evident from inspection of panel A. In panel A, there are six curves presented, two for each concentration; each data point is represented by a dot (approximately 200 points per concentration), and a solid line represents the values predicted from the fit. The agreement is clear. That the fit does not show systematic error is demonstrated in panel B. The difference between the data values and the fit values is presented for each cell. The residuals are small in value (root mean square deviation error = 0.0013), are approximately randomly distributed about zero, and are of the same order in all three cells. Fits of this quality are typical of all the data sets reported here. In considering these data, it is worth noting that the K_a from the fit yields a K_d of 1.9×10^{-7} M, meaning that the tubulin was approximately 40%, 30%, and 20% dissociated in cells 1, 2, and 3, respectively. That a single K_a value predicts equally well (see Figure 1B) the concentration distribution in cells with three different tubulin concentrations (corresponding, in this case, to 20–40% dissociation) provides clear evidence for a single equlibrium between the tubulin dimer and its monomers.

Table I: Effect of Colchicine, GDP, and GTP on Tubulin Dimer Formation at 4.5 °C

K_a	ln K_a[a]	$10^{-6}K_a$ (M^{-1})	$10^{-6}K_a$ av (M^{-1})	10^7K_d (M)
expected[b]	15.40	4.9	4.9	2.0
found	15.39	4.8	4.8	2.1
+colchicine	16.63, 16.98	16.7, 23.7	20.0	0.5
+GDP	16.68, 16.49	17.5, 14.5	16.0	0.6
+GTP	15.46, 15.61	5.2, 6.0	5.6	1.8

[a] Except as noted, values are the results of fitting data from separate ultracentrifuge runs as in Figure 2. [b] Calculated by using eq 5 and $\Delta H°$ and $\Delta S°$ values from Figure 3.

Effect of Colchicine, GDP, and GTP on the Equilibrium. Since a previous report (Detrich et al., 1982) presented evidence that colchicine stabilizes the tubulin dimer against dissociation, we examined the effect of certain molecules on tubulin monomer–dimer equilibrium. For these experiments, tubulin complexed with the test molecules was prepared as described under Materials and Methods and centrifuged to equilibrium, and data were fitted as in Figure 2. The results of this series of experiments are presented in Table I. As indicated, at the temperature chosen for these experiments (4.5 °C), the expected (see below and Table I) and observed K_a for dimer formation was about 4.9×10^6 M^{-1} ($K_d = 2 \times 10^{-7}$ M). Colchicine stabilized the dimer, increasing the K_a to about 20×10^6 M^{-1}, slightly more than the 3-fold stabilization reported by Detrich et al. (1982). Tubulin–GDP, prepared by the exchange procedure under Materials and Methods, also exhibited enhanced dimer stability, shown by an approximately 3-fold increase in K_a to about 16×10^6 M^{-1}. If GTP was substituted for GDP in the preparation, little change was noted compared to standard conditions.

Temperature Dependence of Equilibrium. A series of sedimentation equilibrium experiments were designed to examine the temperature dependence of the equilibrium. Each was a three-cell, three-concentration, three-radii experiment at a single temperature, with a simultaneous fit for the K_a, as in Figure 2. The results of these experiments, covering the temperature range 2–30 °C, are presented in Figure 3 in the form of a van't Hoff plot. The natural logarithm of the K_a, which is the quantity that the fitting actually yields (see

Materials and Methods), is plotted against the reciprocal of the thermodynamic (absolute) temperature.

The data of Figure 2 were analyzed according to the relation

$$\ln K_a = \Delta S°/R - (\Delta H°/R)(1/T) \quad (5)$$

which can be derived directly from

$$\Delta G° = -RT \ln K \quad (6)$$

and

$$\Delta G° = \Delta H° - T\Delta S° \quad (7)$$

From eq 5, it can be seen that the entropy change can be obtained from the intercept and the enthalpy change from the slope of the van't Hoff plot, providing it is linear. If it is not linear, the nonlinearity will be due to the variation of $\Delta H°$ with temperature, a reflection of a difference in heat capacity $\Delta C_p°$ between the monomers and the dimer. In the case that $\Delta C_p°$ is not zero, the data can be fitted to a quadratic equation in $1/T$, whereas if $\Delta C_p°$ is zero, a linear fit to the data will be applied.

A linear fit to the data was performed and is shown as the solid line in Figure 3. The root mean square deviation error for this fit was 0.154. From eq 5, this fit yielded values for the entropy change on association, $\Delta S° = 38.1 \pm 2.4$ cal deg^{-1} mol^{-1}, and values for the enthalpy change on association, $\Delta H° = 2.08 \pm 0.7$ kcal mol^{-1}. These values yield (eq 7) standard free energy changes on association, $\Delta G°$, of −8.5 kcal mol^{-1} at 4 °C and −9.5 kcal mol^{-1} at 30 °C.

A number of attempts were made to fit these data to a quadratic to test for curvature, and hence nonzero $\Delta C_p°$. These were judged unsuccessful since the determination coefficient R^2 was decreased and the root mean square deviation error was increased compared to the linear fit and the quadratic term always had a standard error of the estimate larger than the estimated value of this term. Attempts to estimate $\Delta C_p°$ by the fitting procedure of Lee and Timasheff (1977) gave similar results (best estimate: 1.8 ± 4.6 cal deg^{-1} mol^{-1}). Therefore, the linear fit was accepted, with the attendant conclusion that the $\Delta C_p°$ was small in value and not reliably distinguishable from zero.

Salt Dependence of the Equilibrium. The data in Figure 3 demonstate the importance of entropic forces in the formation of the dimer. Both hydrophobic interactions and ionic (charge-neutralizing) interactions can contribute to positive entropic change on association (Ross & Subramanian, 1981). In order to distinguish these two types of interactions, we examined the effect of an elevated concentration of salt on the monomer–dimer equilibrium. We tested 0.25 M NaCl for its ability to alter the association constant derived from three-cell experiments such as Figure 2. This concentration of added NaCl is sufficient to suppress completely MAP-induced polymerization of tubulin, presumably by inhibiting MAP–tubulin interaction (Olmsted & Borisy, 1975; Bhattacharyya et al., 1985). In addition, this concentration of added NaCl results in ca. 4-fold reduction in polymerization (at 37 °C) of purified rat brain tubulin (Bhattacharyya et al., 1985) and a ca. 4-fold increase in the critical concentration for polymerization (at 10 °C) of Antarctic fish tubulin, corresponding to a ca. 10% reduction in the $\Delta G°$ (Detrich et al., 1989).

As shown in Table II, this concentration of added salt had little effect on the association equilibrium. This is best seen by examining the effect on the free energy of association, $\Delta G°$. The presence of 0.25 M NaCl reduced the $\Delta G°$ in both of two experiments, but the reduction represented only 3–5% of the free energy change on association of monomers to form the dimer. Thus, the contribution of ionic interactions to the positive entropy change on association must be small, and we conclude that hydrophobic interactions must predominate. In contrast, the MAP–tubulin association is significantly stabilized by ionic interactions, whereas the tubulin dimer–dimer association (for both rat and Antarctic fish tubulins) is intermediate in salt sensitivity (Bhattacharyya et al., 1985; Detrich et al., 1989).

Discussion

Data presented in this paper demonstrate that the rat brain tubulin $\alpha\beta$ dimer exists in equilibrium with its dissociated α and β monomers, in agreement with previous reports for rat brain tubulin (Sackett et al., 1989a, 1990) and bovine brain tubulin (Detrich & Williams, 1978; Detrich et al., 1982; Mejillano & Himes, 1989). Furthermore, the association constant from this equilibrium study is in good agreement with that previously obtained by a kinetic method (Sackett et al., 1989a): 4.9×10^6 M^{-1}, giving a K_d of 2×10^{-7} M, compared with a K_d of 1.5×10^{-7} M from the previous study, both at 5 °C.

As mentioned earlier, however, there is some disagreement with values from other studies with bovine brain tubulin using equilibrium ultracentrifugation (Detrich & Williams, 1978; Detrich, et al., 1982) or fluorescence anisotropy (Mejillano & Himes, 1989) and with rat brain tubulin using fluorescence of Nile Red (Sackett et al., 1990); these studies yielded K_d values of $(8–10) \times 10^{-7}$ M. The explanation of these differences is not clear to us. Preliminary studies with bovine brain tubulin (performed as in Figure 2) yield results comparable to those of rat brain tubulin (unpublished), suggesting that species differences are not the cause. Differences in preparation, storage, or technique may be the cause, as any of these may have led to subtle structural changes. In arriving at the constants reported here, the data were fitted to a model containing terms for monomer and dimer only (see eq 4 under Materials and Methods). No term was included for higher order assemblies such as tetramers, and inclusion of such terms did not improve the fit (data not shown). If significant amounts of tetramer were present, it would be seen as a systematic deviation from the fit: residuals increasing with increasing protein concentration. No such deviation was seen (Figure 2). The previous workers (Detrich et al., 1982) *did* require such a term and estimated the K_a (dimer to tetramer) as ca. 4×10^3 M^{-1}. The protein concentrations used here were lower than those in the previous study (the highest concentration here, 3×10^{-6} M, approximates the lowest concentration there). Thus, if the K_a derived by Detrich et al. is accepted, the maximum amount of tetramer in our samples would not be more than about 1% by weight, a level we cannot rule out. In our earliest experiments we also used longer solution columns as had Detrich et al. (which required up to 15 h to establish equilibrium), and under such conditions it was necessary to include a term for an oligomer larger than dimer (data not shown), suggesting that these forms may appear during the run as the protein ages. Use of the short column, fast run time system reported here obviated the need for these terms.

The tubulin dimer is stabilized against dissociation by the presence of bound colchicine, as demonstrated by the ca. 4-fold increase in K_a obtained for the tubulin–colchicine complex compared to tubulin alone. The dimer is also stabilized against dissociation by the presence of bound GDP: the K_a for tubulin–GDP is about 3-fold higher than for tubulin–GTP. Thus, in addition to the well-known ability of colchicine and GDP to prevent tubulin from polymerizing, these agents share the property of enhancing dimer formation. Furthermore,

Table II: Salt Effects on Thermodynamics of Dimer Formation

	ln K_a	$\Delta G°$ [b] (kcal)	found/ expected (%)
run 1 (temp = 3.8 °C)			
expected[a] (0 M NaCl)	15.39	−8.46	
found (0.25 M NaCl)	14.68	−8.07	95.4
run 2 (temp = 6.8 °C)			
expected[a] (0 M NaCl)	15.43	−8.58	
found (0.25 M NaCl)	14.98	−8.33	97.1

[a] Calculated by using eq 5 and $\Delta H°$ and $\Delta S°$ values from Figure 3. [b] Calculated as $\Delta G° = -RT \ln K_a$.

there is evidence that both of these agents may bind to the β subunit of the tubulin dimer (Nath & Himes, 1986; Hesse et al., 1987; Roach et al., 1985; Wolff et al., 1991). Could it be that the promotion of dimerization (and inhibition of polymerization) afforded by colchicine and GDP reflect similar change(s) in the conformation of β tubulin induced by these agents? Further study may resolve this question.

The temperature dependence of the K_a for dimer formation, presented in Figure 3, yields positive values for both the enthalpy and entropy change on association, 2.1 kcal mol^{-1} and 38.1 cal deg^{-1} mol^{-1}, respectively. These values suggest the importance of hydrophobic interactions in the formation of the dimer (Ross & Subramanian, 1981). These hydrophobic interactions presumably come into play in the approach and joining of the α·N and β·C domain surfaces. While formation of a more ordered final configuration of the protein (fewer degrees of freedom due to dimer formation) would yield a negative entropic change, the net positive $\Delta S°$ suggests the greater importance of hydrophobic interaction in dimer formation. The hydrophobic nature of this contact confirms suggestions based on the fluorescence of bound Nile Red (Sackett et al., 1990) and indicates that this contact is unlikely to involve the highly charged carboxy-terminal "tail" of the subunits (Sackett & Wolff, 1986) and must involve more "internal" regions of the protein, as suggested by cross-linking experiments (Kirchner & Mandelkow, 1985; Serrano & Avila, 1985). Ionic interactions might also have contributed to the positive $\Delta S°$ (Ross & Subramanian, 1981), but the small effect of NaCl on the K_a suggests that this contribution was probably small. This is of note since it has been proposed (Sherman et al., 1983; Yaffe et al., 1988) that the α·N-terminal methionine is involved in a salt-bridge interaction in the dimer. Other protein associations that have similar values for $\Delta H°$ and $\Delta S°$ (i.e., both positive) include trypsin association with modified soybean inhibitor (Baugh & Trowbridge, 1972), calcium–calmodulin association with melittin (Milos et al., 1987), cytochrome c_3–ferredoxin association (Guerlesquin et al., 1987), ricin subunit association (Lewis & Youle, 1986), and, indeed, tubulin dimer association to microtubules (see below).

Nevertheless, these thermodynamic parameters of tubulin dimer formation mark it as an unusual protein–protein interaction. Widely held views to the contrary notwithstanding, available thermodynamic data do not indicate that hydrophobic interactions are commonly the major noncovalent forces stabilizing protein associations. If this were so, thermodynamic studies should find, as here, positive $\Delta H°$ and positive $\Delta S°$ of association. On the contrary, more commonly both values are found to be negative (Ross & Subramanian, 1981). These findings do not indicate the hydrophobic interactions are irrelevant to many protein interactions but rather point to the greater net importance of other interactions, such as van der Waals contacts, hydrogen-bond formation in low dielectric environments (protein interior), and ionic interactions.

In addition to negative $\Delta H°$ and $\Delta S°$, most protein associations are characterized by a (frequently large) negative value of $\Delta C_p°$. The heat capacity change found here for tubulin was small or zero, which is unusual for protein associations, as well as surprising for a hydrophobic interaction. Small or zero $\Delta C_p°$ values have been found for other protein associations, such as the dimerization of rabbit muscle phosphofructokinase (Luther et al., 1986), ricin subunit association, which also exhibits positive $\Delta H°$ and $\Delta S°$ (Lewis & Youle, 1986), and, again, the association of tubulin dimers to form microtubules (see below).

Similar results (positive $\Delta H°$ and $\Delta S°$, small or zero $\Delta C_p°$) have been obtained in thermodynamic studies of polymerization of pure (MAP-free) tubulin from porcine brain (Robinson & Engelborghs, 1982), Antarctic fish brain (Williams et al., 1985; Detrich et al., 1989), or sea urchin eggs (Detrich et al., 1989). Thus, both the association of tubulin monomers and the association of tubulin dimers are entropically driven (with positive $\Delta H°$ and $\Delta S°$) and are dominated by hydrophobic interactions.

These similarities invite further comparison, but such a comparison is not without its difficulties since the monomer–dimer system is a reversible equilibrium whereas the dimer–polymer system is not, due to hydrolysis of GTP. In addition, polymerization involves the formation of more than one type of contact. Regarding the GTP hydrolysis, it has been pointed out that this is not thermodynamically coupled to elongation (and therefore dimer–dimer contact formation) since nonhydrolyzable analogues of GTP give nearly identical critical concentrations (Detrich et al., 1989).

Regarding the formation of more than one contact in polymerization, dimers do establish both longitudinal (along the protofilament) and lateral contacts in the polymer,[3] but these two are not equivalent. Electron microscopic observations of intact (Erickson, 1974; Amos, 1982) and frayed microtubules (showing intact, separate protofilaments) demonstrate that longitudinal contacts are stronger than lateral ones (Erickson, 1974; Kirschner & Williams, 1974; Warfield & Bouck, 1974; Mandelkow & Mandelkow, 1985). Numerical modeling of tubulin sheets and microtubules indicates that the longitudinal contacts are 5–10 times stronger than the lateral ones (Erickson & Pantaloni, 1981; Voter & Erickson, 1984). Cross-linking studies have shown that this contact is between the amino-terminal domain of β tubulin (β·N) and the carboxy-terminal domain of α tubulin (α·C) (Kirchner & Mandelkow, 1985). Thus, the energetics of polymerization will largely reflect the energetics of foramation of the α·C–β·N contact. The similarity in the thermodynamic parameters for dimer formation and for polymer formation may, therefore, reflect a similarity in the properties of the surfaces forming the α·N–β·C monomer–monomer contact in the dimer and the α·C–β·N dimer–dimer contact in the polymer.[4]

We conclude that both microtubule formation and dimer formation are entropically driven interactions, favored by

[3] The tubulin dimer has dimensions of ca. 5 × 8 nm (Amos, 1982; Bhattacharyya et al., 1985; Sackett & Wolff, 1986). Dimer association along the longer axis results in formation of protofilaments. The contacts involved in this association are termed longitudinal contacts. The contacts between dimers in adjacent protofilaments are established along the shorter axis of the dimer and are termed lateral contacts.

[4] Despite the similarities between the surfaces forming these contacts, there are clearly differences. The two contacts differ in salt sensitivity, as mentioned above. In addition, the values of $\Delta S°$ and $\Delta H°$, though positive for both contacts, are different, resulting in the well-known temperature sensitivity of polymer formation and the much reduced temperature sensitivity of dimer formation demonstrated here.

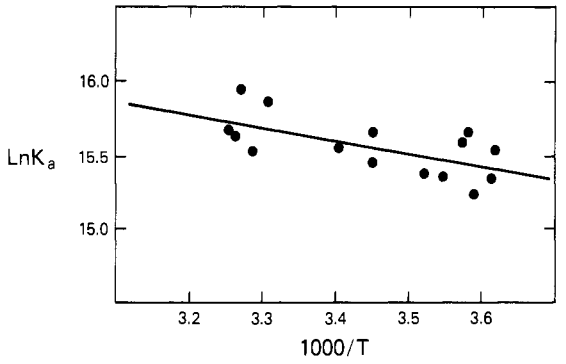

FIGURE 3: Temperature dependence of the equilibrium. A number of three-cell experiments like that shown in Figure 1 have been performed over the temperature range of 2–30 °C. A van't Hoff plot of the data is shown. Each data point represents one three-cell run. The data are presented as the natural logarithm of the best fit estimate of the K_a plotted versus the reciprocal of absolute temperature. The solid line represents the best linear fit to the data. Root mean square deviation error for this fit = 0.154.

hydrophobic interactions. Despite the unusual nature of these two associations, their similarity may be understood in light of the homologous nature of the protein surfaces involved. Thus, the surface of the α·N domain involved in monomer–monomer interaction with β·C is homologous to the β·N domain surface involved in dimer–dimer interaction with α·C. The similarity of the major noncovalent forces contributing to the stability of associations made on those surfaces may be a reflection of the structural similarity.

ACKNOWLEDGMENTS

We thank Dr. J. Wolff for many helpful discussions and continuing support during the course of this work and for critical reading and discussions of the manuscript.

Registry No. GDP, 146-91-8; GTP, 86-01-1; colchicine, 64-86-8.

REFERENCES

Amos, L. A. (1982) in *Electron Microscopy of Proteins* (Harris, J. R., Ed.) Vol. 3, pp 207–250, Academic Press, Orlando, FL.

Andersen, K. B., & Vaughan, M. H. (1982) *J. Chromatogr. 240*, 1–8.

Andreu, J. M., & Timasheff, S. N. (1982) *Biochemistry 21*, 6465–6476.

Baugh, R. J., & Trowbridge, C. G. (1972) *J. Biol. Chem. 247*, 7498–7501.

Bhattacharyya, B., Sackett, D. L., & Wolff, J. (1985) *J. Biol. Chem. 260*, 10208–10216.

Christopherson, R. I. (1983) *Methods Enzymol. 91*, 278–281.

Cohn, E. J., & Edsall, J. T. (1943) *Proteins, Amino Acids, and Peptides*, Reinhold, New York.

Correia, J. J., Baty, L. T., & Williams, R. C., Jr. (1987) *J. Biol. Chem. 262*, 17278–17284.

Croom, H. B., Correia, J. J., Baty, L. T., & Williams, R. C., Jr. (1985) *Biochemistry 24*, 768–775.

Detrich, H. W., III, & Williams, R. C., Jr. (1978) *Biochemistry 17*, 3900–3907.

Detrich, H. W., III, Williams, R. C., Jr., & Wilson, L. (1982) *Biochemistry 21*, 2392–2400.

Detrich, H. W., III, Johnson, K. A., & Marchese-Ragona, S. P. (1989) *Biochemistry 28*, 10085–10093.

Erickson, H. P. (1974) *J. Supramol. Struct. 2*, 393–411.

Erickson, H. P., & Pantaloni, D. (1981) *Biophys. J. 34*, 293–309.

Guerlesquin, F., Sari, J. C., & Bruschi, M. (1987) *Biochemistry 26*, 7438–7443.

Hamel, E., & Lin, C. M. (1984) *Biochemistry 23*, 4173–4184.

Hesse, J., Thierauf, M., & Ponstingl, H. (1987) *J. Biol. Chem. 262*, 15472–15475.

Himes, R. H., Burton, P. R., & Gaito, J. M. (1977) *J. Biol. Chem. 252*, 6222–6228.

Kirchner, K., & Mandelkow, E.-M. (1985) *EMBO J. 4*, 2397–2402.

Kirschner, M. W., & Williams, R. C. (1974) *J. Supramol. Struct. 2*, 412–428.

Lee, J. C., & Timasheff, S. N. (1977) *Biochemistry 16*, 1754–1764.

Lee, J. C., Frigon, R. P., & Timasheff, S. N. (1973) *J. Biol. Chem. 248*, 7253–7262.

Lewis, M. S., & Youle, R. J. (1986) *J. Biol. Chem. 261*, 11571–11577.

Luther, M. A., Cai, G.-Z., & Lee, J. C. (1986) *Biochemistry 25*, 7931–7937.

Mandelkow, E.-M., & Mandelkow, E. (1985) *J. Mol. Biol. 181*, 123–135.

Mejillano, M. R., & Himes, R. H. (1989) *Biochemistry 28*, 6518–6524.

Milos, M., Schaer, J.-J., Comte, M., & Cox, J. A. (1987) *J. Biol. Chem. 262*, 2746–2749.

Nath, J. P., & Himes, R. H. (1986) *Biochem. Biophys. Res. Commun. 135*, 1135–1143.

Olmsted, J. B., & Borisy, G. G. (1975) *Biochemistry 14*, 2996–3005.

Ponstingl, H., Little, M., & Krauhs, E. (1984) *Pept. Protein Rev. 2*, 1–81.

Roach, C., Bane, S., & Luduena, R. (1985) *J. Biol. Chem. 260*, 3015–3023.

Roark, D. E. (1976) *Biophys. Chem. 5*, 185–196.

Robinson, J., & Engelborghs, Y. (1982) *J. Biol. Chem. 257*, 5367–5371.

Ross, P. D., & Subramanian, S. (1981) *Biochemistry 20*, 3096–3102.

Sackett, D. L., & Wolff, J. (1986) *J. Biol. Chem. 261*, 9070–9076.

Sackett, D. L., Zimmerman, D. A., & Wolff, J. (1989a) *Biochemistry 28*, 2662–2667.

Sackett, D. L., Lippoldt, R. E., Gibson, C., & Lewis, M. (1989b) *Anal. Biochem. 180*, 319–325.

Sackett, D. L., Knutson, J. R., & Wolff, J. (1990) *J. Biol. Chem. 265*, 14899–14906.

Serrano, L., & Avila, J. (1985) *Biochem. J. 230*, 551–556.

Shelanski, M. L., Gaskin, F., & Cantor, C. R. (1973) *Proc. Natl. Acad. Sci. U.S.A. 70*, 765–768.

Sherman, G., Rosenberry, T. L., & Sternlicht, H. (1983) *J. Biol. Chem. 258*, 2148–2156.

Sloboda, L., & Rosenbaum, J. L. (1982) *Methods Enzymol. 85*, 409–416.

Teller, D. C. (1973) in *Methods in Enzymology* (Hirs, C. H. W., & Timasheff, S. N., Eds.) Vol. 27, pp 346–441, Academic Press, San Diego, CA.

Voter, W. A., & Erickson, H. P. (1984) *J. Biol. Chem. 259*, 10430–10438.

Warfield, R. K. N., & Bouck, G. B. (1974) *Science 186*, 1219–1221.

Williams, R. C., Jr. (1979) *Methods Enzymol. 61*, 96–103.

Williams, R. C., Jr., Correia, J. J., & DeVries, A. L. (1985) *Biochemistry 24*, 2790–2798.

Wolff, J., Knipling, L., Cahnmann, H. J., & Palumbo, G. (1991) *Proc. Natl. Acad. Sci. U.S.A.* (in press).

Yaffe, M. B., Levison, B. S., Szasz, J., & Sternlicht, H. (1988) *Biochemistry 27*, 1869–1880.